JOC *Article*

Electron-Transfer-Induced Substitution of Alkylated C_{60} Chlorides with Proton Sponge

Yangsoo Lee, Toshikazu Kitagawa,* and Koichi Komatsu*

Institute for Chemical Research, Kyoto University, and CREST, Japan Science and Technology Corporation (JST), Uji, Kyoto 611-0011, Japan

kitagawa@scl.kyoto-u.ac.jp

Received August 2, 2003

A series of alkylated C_{60} chlorides 1,4-$RC_{60}Cl$ (**1**) were found to undergo nucleophilic substitution with 1,8-bis(dimethylamino)naphthalene (**2**), affording 1,4-$RC_{60}Ar$ [**3**, Ar = 4,5-bis(dimethylamino)-1-naphthyl] in good yields. An $S_{RN}1$ mechanism, initiated by a single-electron transfer from **2** to **1**, is proposed on the basis of the enhanced rates compared with the rate of the S_N1 reaction of **1** with anisole. The involvement of free radicals in the reaction is supported by the formation of a small amount of dimer $RC_{60}-C_{60}R$ (**4**) as a byproduct. The enhanced ability of C_{60} chlorides **1** to accept an electron, attributable to the inductive effect of the directly attached chlorine atom, was demonstrated by its reduction potential and calculated LUMO energy.

Introduction

On the basis of its high electron affinity, C_{60} tends to form anionic species under various conditions. In addition to the chemical or electrochemical multielectron reduction to $C_{60}{}^{n-}$,[1] the ease of nucleophilic addition, which produces a stable anion $RC_{60}{}^-$,[2] is a consequence of the inherent electronegativity of the π-conjugated system of the C_{60} cage. On the other hand, halogen atom(s), directly attached to the C_{60} cage, can dramatically affect the chemical behavior of the cage, since compounds having a C(sp^3)−Cl bond can be regarded as carbocation equivalents. It would be logical to expect that chlorine-attached C_{60} could undergo substitution by nucleophiles, rather than addition to the double bond. As a clear example of such a tendency, we recently reported on the S_N1 solvolysis of 1-alkyl-4-chloro-1,4-dihydro[60]fullerenes **1a**−**c** by nucleophilic solvents under mild conditions (Scheme 1).[3] The proposed intermediates, $RC_{60}{}^+$, were independently generated by the ionization of fullerenols RC_{60}-OH in superacidic media and were observed by NMR as long-lived carbocations.[4]

SCHEME 1. S_N1 Reaction of Alkylated C_{60} Chlorides

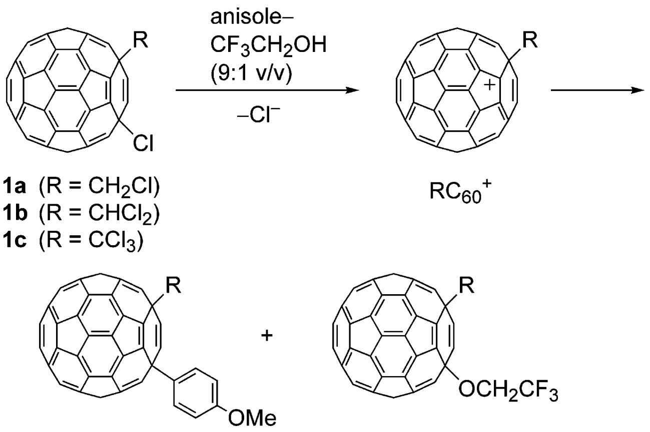

However, when the nucleophile is a good electron donor, substitution may occur by a radical mechanism rather than the classical S_N1 mechanism. The nucleophilic substitution of RX by a radical mechanism induced by single-electron transfer, as outlined in Scheme 2, is known as an $S_{RN}1$ reaction.[5] This reaction is initiated by the reduction of a small amount of RX to its radical anion (eq 1). Its spontaneous dissociation to R$^\bullet$ and X$^-$ (eq 2) and the subsequent transformation of R$^\bullet$ (eqs 3 and 4)

SCHEME 2. $S_{RN}1$ Mechanism

$$\mathrm{RX} + e^- \longrightarrow \mathrm{RX}^{\bullet -} \qquad (1)$$

$$\mathrm{RX}^{\bullet -} \longrightarrow \mathrm{R}^\bullet + \mathrm{X}^- \qquad (2)$$

$$\mathrm{R}^\bullet + \mathrm{Nu}^- \longrightarrow \mathrm{RNu}^{\bullet -} \qquad (3)$$

$$\mathrm{RNu}^{\bullet -} + \mathrm{RX} \longrightarrow \mathrm{RNu} + \mathrm{RX}^{\bullet -} \qquad (4)$$

---

[1] Reed, C. A.; Bolskar, R. D. *Chem. Rev.* **2000**, *100*, 1075.

[2] (a) Murata, Y.; Komatsu, K.; Wan, T. S. M. *Tetrahedron Lett.* **1996**, *37*, 7061. (b) Murata, Y.; Motoyama, K.; Komatsu, K.; Wan, T. S. M. *Tetrahedron* **1996**, *52*, 5077. (c) Komatsu, K.; Murata, Y.; Takimoto, N.; Mori, S.; Sugita, N.; Wan, T. S. M. *J. Org. Chem.* **1994**, *59*, 6101. (d) Fagan, P. J.; Krusic, P. J.; Evans, D. H.; Lerke, S. A.; Johnston, E. *J. Am. Chem. Soc.* **1992**, *114*, 9697. (e) Keshavarz-K, M.; Knight, B.; Srdanov, G.; Wudl, F. *J. Am. Chem. Soc.* **1995**, *117*, 11371. (f) Fukuzumi, S.; Nakanishi, I.; Maruta, J.; Yorisue, T.; Suenobu, T.; Itoh, S.; Arakawa, R.; Kadish, K. M. *J. Am. Chem. Soc.* **1998**, *120*, 6673.

[3] Kitagawa, T.; Lee, Y.; Hanamura, M.; Sakamoto, H.; Konno, H.; Takeuchi, K.; Komatsu, K. *Chem. Commun.* **2002**, 3062.

[4] Kitagawa, T.; Sakamoto, H.; Takeuchi, K. *J. Am. Chem. Soc.* **1999**, *121*, 4298.

[5] (a) Bunnett, J. F. *Acc. Chem. Res.* **1978**, *11*, 413. (b) Rossi, R. A.; Santiago, A. N. *Trends Org. Chem.* **1992**, *3*, 193. (c) Savéant, J.-M. *Tetrahedron* **1994**, *50*, 10117. (d) Rossi, R. A.; Pierini, A. B.; Peñéñory, A. B. In *The Chemistry of Halides, Pseudo-Halides and Azides*; Patai, S., Rappoport, Z., Eds.; Wiley: New York, 1995; pp 1395−1485. (e) Costentin, C.; Hapiot, P.; Medebielle, M.; Savéant, J.-M. *J. Am. Chem. Soc.* **1999**, *121*, 4451.

10.1021/jo0351421 CCC: \$27.50

SCHEME 3. Reaction of 1 with 2

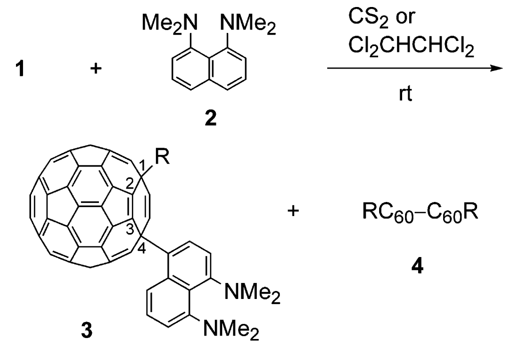

a: R = CH_2Cl, **b**: R = $CHCl_2$, **c**: R = CCl_3

TABLE 1. Yields of Substitution Product 3 and Dimer 4 in the Reaction of 1 with 2[a]

		product (yield, %)[c]	
substrate[b]	time (h)	substitution product	dimer
1a	1	**3a** (82)	**4a** (12)
1b	1	**3b** (>90)	**4b** (9)
1c	3	**3c** (>90)	**4c** (trace)

[a] Reactions were carried out with 50 equiv of **2** in $Cl_2CDCDCl_2$ at ambient temperature in the dark. [b] Initial concentration, 0.5–8.7 × 10^{-3} M. [c] Yields were determined by ^1H NMR integration and analytical HPLC using a Buckyprep column. C_{70} was used as an HPLC internal standard.

constitutes a chain propagation, the net result of which is the substitution of the chlorine atom by the nucleophile. Chlorides **1a**–**c**, with electronegative characteristics, may be subject to this type of substitution by nucleophiles with donating ability. Thus, it would be of interest to study the reaction of alkylated C_{60} chlorides with highly electron-rich aromatic compounds. 1,8-Bis(dimethylamino)naphthalene (proton sponge, **2**)[6] can act as both a nucleophile and an electron donor. In this paper we report on the nucleophilic substitution of **1a**–**c** with **2** as the first example of the $S_{RN}1$ substitution of C_{60} derivatives. Additionally, the products of those reactions are of structural interest because, in these molecules, the C_{60} cage and the donor are connected by a C–C single bond, which is the shortest possible linker.

Results and Discussion

An excess amount of proton sponge **2** was added to a solution of **1** in CS_2 or $Cl_2CHCHCl_2$ at room temperature in the dark, and the reaction was monitored by ^1H NMR. The signals of **1** quickly disappeared with the generation of substitution product **3** within 10 min (Scheme 3). During this period, the color of the solution changed from brown to dark green. The formation of dimer **4** was also detected by HPLC analysis. The yields of the products determined by using $Cl_2CDCDCl_2$ as solvent are listed in Table 1.

For product identification, the solution was diluted with acetone in order to precipitate the C_{60} derivatives. The collected precipitate was dissolved in toluene and further separated by HPLC to afford adduct **3** together with a small amount of dimer **4**.

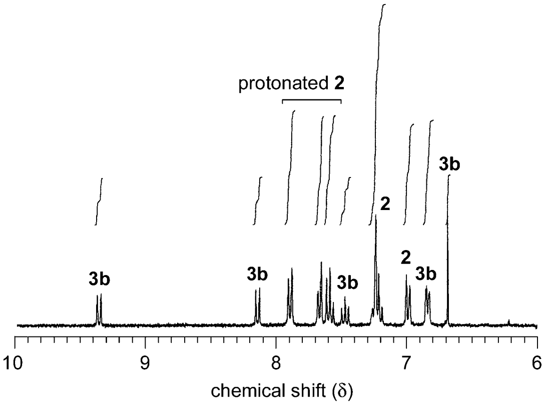

FIGURE 1. Aromatic region of the ^1H NMR spectrum of a solution of **1b** in $Cl_2CDCDCl_2$ 16 min after the addition of **2** (3.4 equiv) at 23 °C.

The structures of the major products **3a**–**c** were determined by the consistent ^1H and ^{13}C NMR spectra, UV–vis absorption spectra, and HRMS data. Five aromatic proton signals and two dimethylamino proton signals are observed in the ^1H NMR spectra, and the coupling pattern of the aromatic region indicates that C-4 of the naphthyl carbon is bonded to C_{60}. The aromatic signals are considerably shifted to lower field relative to those of the parent proton sponge **2** (Figure 1). This can be attributed to the ring current of the C_{60} cage and the partial intramolecular charge transfer from the proton sponge moiety to the C_{60} cage (vide infra). The ^{13}C NMR spectra of **3a**–**c** showed 64–66 sp^2 carbon signals, which correspond to 10 carbons in the naphthalene ring and 58 in the C_{60} cage (2–4 peaks are overlapped). Thus, the molecule has no symmetry, suggesting that the obtained adducts are 1,4-isomers as shown in Scheme 3. This structure is also supported by the absorption band at 448 nm in the UV–vis spectra of **3a**–**c**, which is typical of 1,4-adducts of C_{60} (Figure 2).[7,8]

The proton, released simultaneously with the formation of **3**, was clearly observed by ^1H NMR (Figure 1) in the protonated form of proton sponge (**2**-H^+), which appeared at δ 7.90–7.59 and 3.25. The assignment of these signals was confirmed by measuring the ^1H NMR spectrum of **2** in CS_2–$Cl_2CDCDCl_2$ (4:1) in the presence of added HCl gas. The molar ratio of the produced **3** and protonated **2** was 1:1 throughout the reaction. Thus, when an excess amount of **2** is present, it serves as effective base to trap the acid. No protonated form of adduct **3** was detected, indicating that the generated proton is trapped predominantly by **2**. This suggests a decrease in the basicity of the proton sponge moiety of **3** when it is connected to the C_{60} cage.

Byproducts **4a**–**c** have an exceedingly long HPLC retention time (13.3–14.8 min) compared to that of C_{60} (7.3 min) and **1a**–**c** (6.9–7.5 min), characteristic of dimeric derivatives of C_{60}. Atmospheric pressure chemical

---

[6] (a) Alder, R. W.; Bowman, P. S.; Steele, W. R. S.; Winterman, D. R. *J. Chem. Soc., Chem. Commun.* **1968**, 723. (b) Staab, H. A.; Saupe, T. *Angew. Chem., Int. Ed. Engl.* **1988**, *27*, 865.

[7] (a) Schick, G.; Kampe, K.-D.; Hirsch, A. *J. Chem. Soc., Chem. Commun.* **1995**, 2023. (b) Kadish, K. M.; Gao, X.; Van Caemelbecke, E.; Suenobu, T.; Fukuzumi, S. *J. Phys. Chem. A* **2000**, *104*, 3878.

[8] (a) Kitagawa, T.; Tanaka, T.; Murakita, H.; Nishikawa, A.; Takeuchi, K. *Tetrahedron* **2001**, *57*, 3537. (b) Kitagawa, T.; Tanaka, T.; Murakita, H.; Takeuchi, K. *J. Org. Chem.* **1999**, *64*, 2. (c) Kitagawa, T.; Tanaka, T.; Takata, Y.; Takeuchi, K.; Komatsu, K. *Tetrahedron* **1997**, *53*, 9965.

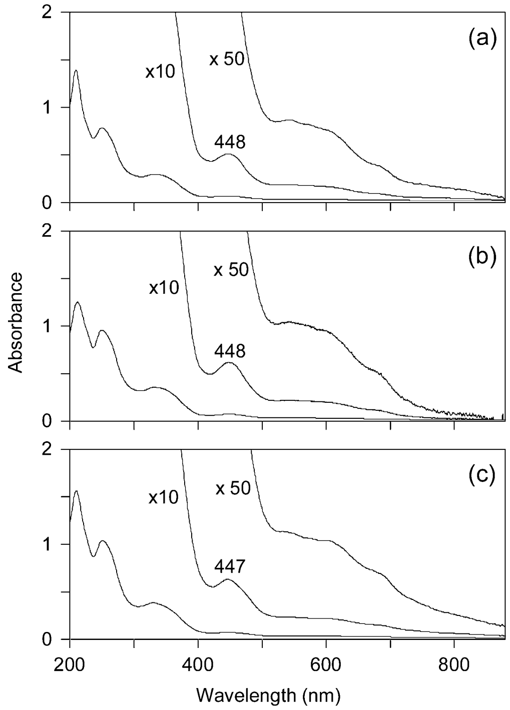

FIGURE 2. UV−vis absorption spectra of **3a**−**c** in cyclohexane (cell length, 1 cm): (a) **3a** (0.76×10^{-5} M); (b) **3b** (1.00×10^{-5} M); (c) **3c** (1.02×10^{-5} M).

SCHEME 4. Proposed Structures of 4

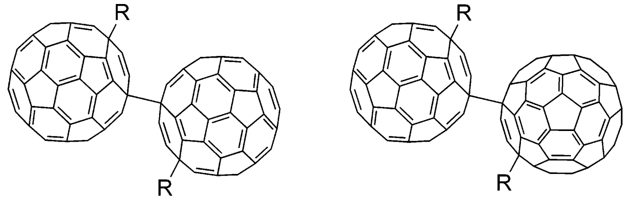

4 (racemic) **4** (meso)

a: R = CH_2Cl, **b**: R = $CHCl_2$, **c**: R = CCl_3

ionization (APCI) mass spectrometry (negative ion mode; solvent, toluene−CH_3OH 1:1) showed signals corresponding to $[(RC_{60})_2 + CH_3O]^-$ and RC_{60}^-, suggesting that **4a**−**c** have the structure $RC_{60}-C_{60}R$, whose C−C bond is readily broken. The ^1H NMR spectra of **4a** showed two AB quartets centered at δ 5.023 ($J = 10.7$ Hz) and 5.028 ($J = 10.8$ Hz) with an intensity ratio of approximately 6:4. This suggests that each C_{60} framework has addends at 1,4 positions, and the product is a mixture of racemic and meso isomers (Scheme 4). Similarly, two singlet peaks (δ 6.98 and 7.06, intensity ratio 6:4) were observed in the ^1H NMR spectrum of **4b**. Bonding of the two components at C-4 in dimers $RC_{60}-C_{60}R$ has been reported for several addends R from the spectroscopic data[7a,9,10] or from the X-ray crystal analysis.[10] Furthermore, the 1-chloronaphthalene solution of **4b** is ESR active, owing to the reversible dissociation of the C−C bond to form a radical $RC_{60}^\bullet$. A weak signal was observed at room temperature, which increased in intensity at higher temperatures. The degree of dissociation was determined to be 0.3% at 423 K using a 1-chloronaphthalene solution of 4-hydoxy-TEMPO as an external standard. A linear plot was obtained between ln(IT) (I = signal intensity) and $1/T$ (Figure 3), based on which the enthalpy of dissociation was determined to be 18.0 kcal/mol, a value close to those reported for $RC_{60}-C_{60}R$ [R = $PO(OEt)_2$, CCl_3, and CBr_3].[11]

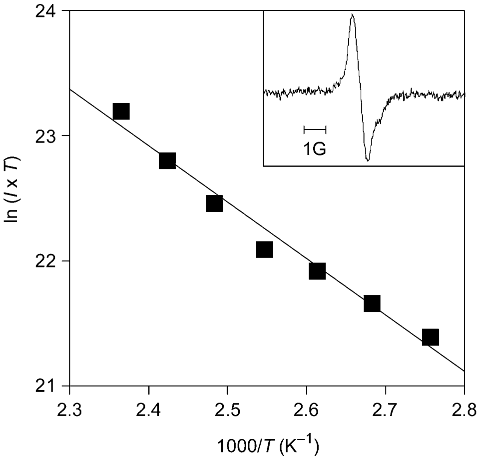

FIGURE 3. Temperature dependence of the signal intensity of the ESR spectra of **4b** in 1-chloronaphthalene. The inset shows the spectrum recorded at 413 K. I denotes the signal intensity (arbitrary unit) obtained by the double integration of the ESR spectrum.

For the kinetic study of the reaction of Scheme 3, the decay of **1b** in the presence of 70 equiv of **2** in $CS_2-Cl_2CDCDCl_2$ (85:15) was monitored by ^1H NMR spectroscopy at −40 °C. A good linear first-order plot was obtained until 2.5 half-lives with a pseudo-first-order rate constant of 2.1×10^{-4} s^{-1}. Although this reaction is a formal nucleophilic substitution, this rate constant is unexpectedly large for such a reaction, considering that **1b** undergoes an S_N1 reaction in anisole−trifluoroethanol (9:1 v/v) much more slowly ($k_1 = 1.5 \times 10^{-5}$ s^{-1}) even at 25 °C.[3] In addition, the S_N1-type reaction of **1** does not occur in pure anisole, being feasible only in polar solvents (i.e., with a high solvent ionizing power) that stabilize the cationic intermediate. When proton sponge **2** was used, however, the same chlorides rapidly reacted even in relatively nonpolar solvents such as CS_2 and 1,1,2,2-tetrachloroethane. It is evident that some process other than S_N1 reaction is responsible for the rate enhancement. A plausible mechanism, which is consistent with the high acceptor and donor abilities of **1** and **2**, is proposed in Scheme 5.

The initial step of the reaction is an electron transfer from **2** to **1**, which forms an ion pair $\mathbf{2}^{\bullet+}\mathbf{1}^{\bullet-}$ (eq 5). Chloride ion would be readily released from $\mathbf{1}^{\bullet-}$ by the cleavage of the C−Cl bond (eq 6, step a), affording an alkylated C_{60} radical $\mathbf{5}^\bullet$.[13] This radical can be reduced by a second molecule of **2** to form an anion $\mathbf{5}^-$ (step b). This step should be feasible, because alkylated C_{60} radicals $RC_{60}^\bullet$ are considered to be efficient oxidants owing to the high

---

[9] Yoshida, M.; Sultana, F.; Uchiyama, N.; Yamada, T.; Iyoda, M. *Tetrahedron Lett.* **1999**, *40*, 735.

[10] Cheng, F.; Murata, Y.; Komatsu, K. *Org. Lett.* **2002**, *4*, 2541.

[11] Enthalpy of dissociation (kcal/mol) of $RC_{60}-C_{60}R$: 17.0 [R = $PO(OEt)_2$[10]], 17.1 (R = CCl_3[12]), 17.0 (R = CBr_3[12]).

[12] (a) Morton, J. R.; Preston, K. F.; Krusic, P. J.; Wasserman, E. *J. Chem. Soc., Perkin Trans. 2* **1992**, 1425. (b) Morton, J. R.; Preston, K. F.; Krusic, P. J.; Hill, S. A.; Wasserman, E. *J. Am. Chem. Soc.* **1992**, *114*, 5454.

SCHEME 5. Plausible Mechanism for the Substitution of 1 with 2

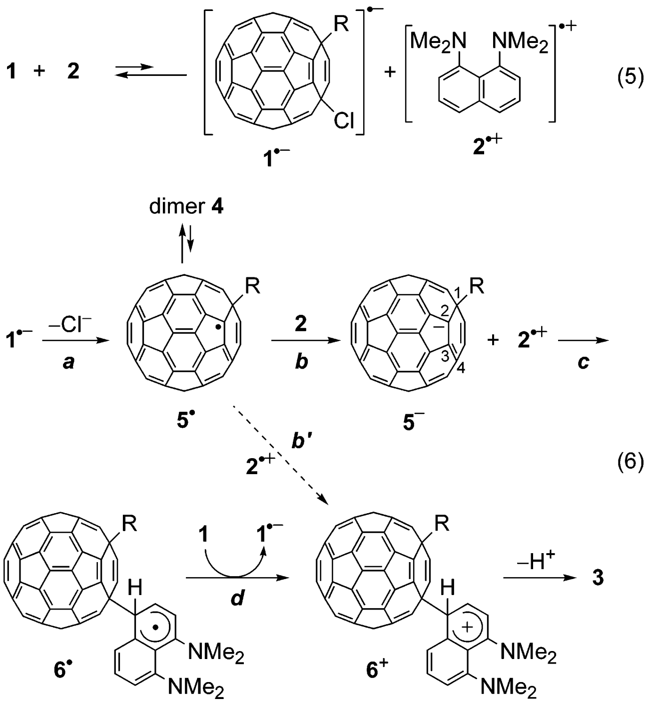

SCHEME 6. $S_{RN}1$ Chain Propagation Step (along with the Termination by the Dimerization of $5^{\bullet}$)

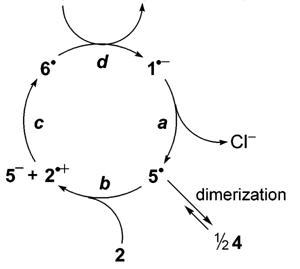

stability of the corresponding anion RC_{60}^-, and, as a result, would be expected to be highly susceptible to reduction by **2**.[14] The produced ion pair, $\mathbf{5}^- + \mathbf{2}^{\bullet+}$, would readily undergo C−C bond formation (step c) to give a radical $\mathbf{6}^{\bullet}$. This radical is reoxidized in step d by **1** to give $\mathbf{6}^+$, which, after deprotonation, eventually affords the final product **3**. The radical anion $\mathbf{1}^{\bullet-}$ is regenerated in step d, making the sequence of eq 6 an $S_{RN}1$ chain propagation. The net reaction, as illustrated in Scheme 6 in the cyclic form, is the conversion of **1** and **2** to **3** and HCl. The electron transfer in eq 5 is the initiation step, which supplies a small amount of $\mathbf{1}^{\bullet-}$ for the initiation of the propagation. As an alternative possibility, the formation of cation $\mathbf{6}^+$ by the direct coupling of $\mathbf{5}^{\bullet}$ and $\mathbf{2}^{\bullet+}$ (Scheme 5, step b′) is also conceivable. In this case, the whole process is a nonchain reaction, where the stoichiometric formation of $\mathbf{2}^{\bullet+}$ by eq 5 is required.

The involvement of radical $\mathbf{5}^{\bullet}$ in the proposed mechanism is supported by the formation of dimer **4** as a byproduct. Since the dimerization of $\mathbf{5}^{\bullet}$ is in competition with its reduction by **2** (step b), it is expected that the product ratio **4**/**3** would change largely with the variation of the concentration of **2**. With 50 equiv of **2b**, chloride **1b** gave only 9% of dimer **4b**, due to the preferential formation of adduct **3b**. By reducing the amount of **2** to 1 equiv, the yield of **4b** increased to 56% (Table 2).[16] Thus, when a large excess of **2** is present, radical $\mathbf{5}^{\bullet}$ is effectively trapped by **2** and a considerable part (but not necessarily all) of the reaction proceeds via pathway b → c → d rather than the direct step b′.

TABLE 2. Effect of Proton Sponge 2 on the Yield of Dimer 4b in the Reaction of 1b with 2[a]

molar ratio of **2**/**1b**	yield of **4b**[b] (%)
1.0	56
2.0	49
4.0	41
7.9	33
16	28
50	9

[a] Reactions were carried out in CS_2 at room temperature for 2 h with initial concentration of **1b** of 2.35×10^{-3} M. [b] Yield was determined by HPLC using a Buckyprep column. C_{70} was used as an internal standard.

The combination of $\mathbf{5}^-$ and $\mathbf{2}^{\bullet+}$ (step c) determines the regioselectivity. The exclusive formation of 1,4-adducts is the result of the balance between the electron distribution of $\mathbf{5}^-$ and the steric repulsion between the two groups attached on the C_{60} framework. Although anions RC_{60}^- have been reported to have the greatest negative charge density and HOMO coefficient at C-2,[8c] the bulkiness of the chloroalkyl group at C-1 appears to prohibit C−C bond formation at C-2. It is probable that a bond is formed at the C-4 position, which is the next most reactive. Observations of similar regioselectivities have been reported for the formation of adducts $RC_{60}R'$ by C−C bond formation between RC_{60}^- and sterically demanding carbocations R'^{+}.[8,17]

It should be noted that although the initiation step (Scheme 5, eq 5) is an endergonic process (based on the redox potentials, vide infra), it occurred thermally without photoexcitation. The inductive effect of the chlorine atom directly attached to the C_{60} core should amplify the electron affinity of **1**. In fact, the LUMO energy level of **1b** (−3.52 eV), calculated by the DFT method (the B3LYP/6-31G* level of theory) is lower by −0.29 eV, compared with that of pristine C_{60}. Consistent with this is the cyclic voltammograms of **1a**−**c** (Figure 4), which demonstrate the first reduction peaks as irreversible waves at $E_p^{red}(1) = -0.71, -0.60$, and −0.71 V, respectively, vs the ferrocene/ferrocenium (Fc/Fc$^+$) couple (Table 3). These values are ca. 0.5 V less negative than the first

---

[13] The initial products of the C−Cl bond cleavage may also be a fullerene anion $\mathbf{5}^-$ and $Cl^{\bullet}$, as proposed for the cleavage of $Ph_5C_{60}Cl^{\bullet-}$: Birkett, P. R.; Taylor, R.; Wachter, N. K.; Carano, M.; Paolucci, F.; Roffia, S.; Zerbetto, F. *J. Am. Chem. Soc.* **2000**, *122*, 4209. However, this would result in immediate electron transfer to form $\mathbf{5}^{\bullet}$ and Cl^-, due to the strong oxidizing ability of $Cl^{\bullet}$.

[14] For example, $CH_3(CH_2)_5C{\equiv}CC_{60}^-$ and t-BuC_{60}^- are reported to have reduction potentials of −0.32 V[2b] and −0.37 V,[15] respectively, vs Fc/Fc$^+$.

[15] Lerke, S. A.; Evans, D. H.; Fagan, P. J. *J. Electrochem. Soc.* **1997**, *144*, 4223.

[16] The difference in the yields of dimers seen in Table 1 is consistent with this result, because the chlorine atoms in R stabilize $\mathbf{5}^-$, making path b more favorable as compared to the dimerization of $\mathbf{5}^{\bullet}$.

[17] Kitagawa, T.; Tanaka, T.; Takata, Y.; Takeuchi, K.; Komatsu, K. *J. Org. Chem.* **1995**, *60*, 1490.

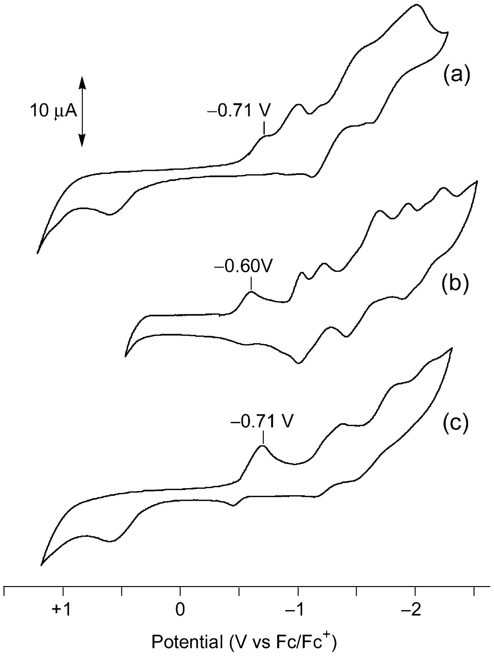

FIGURE 4. Cyclic voltammograms of (a) **1a**, (b) **1b**, and (c) **1c** in 1,2-dichlorobenzene at 23 °C.

TABLE 3. Redox Potentials of C_{60} and Its Derivatives 1 and 3 and Aromatic Amines 2 and 7[a]

		potential (V vs Fc/Fc$^+$)[b]	
compound	solvent	$E^{red}(1)$[c]	$E_p^{ox}(1)$[d]
C_{60}	1,2-$C_6H_4Cl_2$	−1.09, −1.17[e] (rev)	
	PhCN	−0.88 (rev)[f]	
1a	1,2-$C_6H_4Cl_2$	−0.71 (irrev)	
1b	1,2-$C_6H_4Cl_2$	−0.60 (irrev)	
1c	1,2-$C_6H_4Cl_2$	−0.71 (irrev)	
2	PhCN		−0.01 (irrev)
7	PhCN		+0.40 (irrev)
3a	PhCN	−0.96 (rev)	+0.10 (irrev)
3b	PhCN	−0.93 (rev)	+0.10 (irrev)
3c	PhCN	−0.93 (rev)	+0.10 (irrev)

[a] Scan rate, 50 mV/s; supporting electrolyte, 0.05 M $Bu_4N^+PF_6^-$ (for C_{60} and **1**) or 0.05 M $Bu_4N^+BF_4^-$ (for **2**, **7**, and **3**). [b] rev: reversible. irrev: irreversible. Peak potentials and half-wave potentials are listed for reversible and irreversible waves, respectively, unless otherwise noted. [c] First reduction potential. [d] First oxidation potential. [e] Reduction peak potential. [f] Reference 18; supporting electrolyte, 0.1 M $Bu_4N^+ClO_4^-$.

reduction peak potential of C_{60} [$E_p^{red}(1) = -1.17$ V vs Fc/Fc$^+$] measured under the same conditions. The voltammograms showed waves by further reduction processes in the more negative region.

The high donor ability of proton sponge **2** is also demonstrated by its low oxidation potential $E_p^{ox}(1) = -0.01$ V vs Fc/Fc$^+$ (Table 3). A related amine *N*,*N*-dimethyl-1-naphthylamine **7**, having only one dimethylamino group, exhibited a somewhat weaker donor ability [$E_p^{ox}(1) = +0.40$ V]. Although **1b** was found to react with **7** (3.3 equiv) to form an adduct **8** in 44% isolated yield (Scheme 7), the reaction was much slower ($k_1 = 2.4 \times 10^{-4}$ s^{-1} at 23 °C) than the reaction with **2**.

Products **3a**−**c** are donor−acceptor dyads constructed by the C_{60} cage directly bonded to the proton sponge moiety. These adducts showed an irreversible oxidation wave owing to the proton sponge and reversible reduction waves related to the RC_{60} moiety (Table 3). The oxidation potential is 0.11 V shifted to the positive side compared to the potential of proton sponge **2**, and the first reduction potential is slightly (0.05−0.08 V) more negative than the potential of C_{60}. These shifts can be attributed to the electron withdrawing property of the C_{60} framework. According to DFT calculations (the B3LYP/6-31G* level of theory), the HOMO and HOMO-1 of **3b** are localized on the proton sponge moiety and the LUMO and LUMO+1 on the C_{60} framework (Figure 5). The HOMO energy level is 0.27 eV lower than that of **2**, while the LUMO energy level is slightly (0.06 eV) higher than that of pristine C_{60} (Figure 6). These changes in the calculated energy levels are in accord with the observed shift of redox potentials and are interpreted as indicating that the HOMO of proton sponge and the LUMO of C_{60} in **3** interact only slightly.

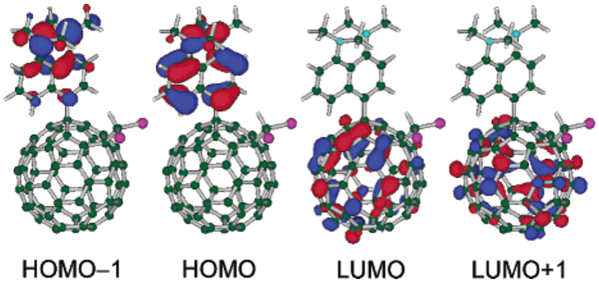

FIGURE 5. Optimized structure and molecular orbitals of **3b** calculated at the B3LYP/6-31G(d) level.

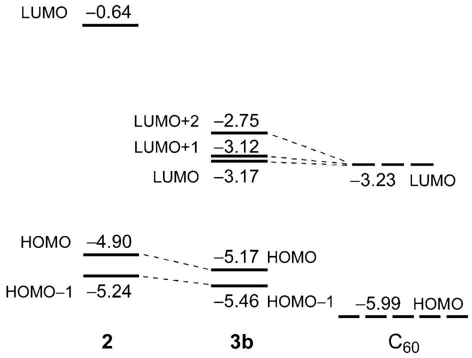

FIGURE 6. Molecular orbital energies of **2**, **3b**, and C_{60} calculated at the B3LYP/6-31G(d) level.

SCHEME 7. Substitution of 1b with 7

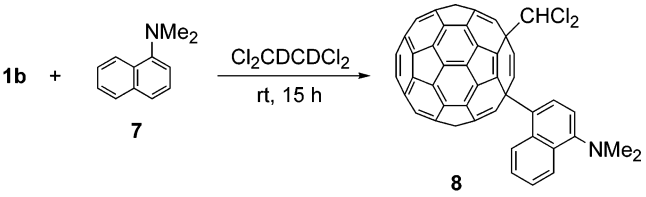

The colors of **3a**−**c** are dark green both in solid state and in solution. This color is unusual for neutral C_{60} derivatives, which are usually brownish or yellowish in solution, and is somewhat similar to that of its anions. This is due to a broad absorption at 610 nm, or 2.0 eV (Figure 2), which can be interpreted as the result of intramolecular charge transfer from the proton sponge moiety to the C_{60} cage. The sum of the atomic Mulliken charges for the proton sponge moiety of **3b**, obtained by the B3LYP/6-31G(d) level, is +0.15.

In conclusion, we demonstrate here that a chlorine atom directly attached to the C_{60} cage in **1a**−**c** is substituted with proton sponge by a mechanism induced by an electron transfer. This is the first example of the $S_{RN}1$ reaction observed for alkylated C_{60} chlorides and is in contrast to our previous observation that the same compounds undergo nucleophilic substitution with anisole by the S_N1 mechanism. Although both mechanisms lead to similar products, they proceed via significantly different elementary steps. Thus, the previously unknown S_N1-$S_{RN}1$ mechanistic dichotomy in the nucleophilic substitution of C_{60}−Cl bond has been revealed. The latter mechanism is what is reasonably anticipated from the inherent electronegativity of fullerenes and is considered to be generally suited to the synthesis of fullerene-donor dyads using a variety of electron-rich nucleophilic molecules.

Experimental Section

Materials. NMR spectra were recorded on 400 and 300 MHz instruments in CS_2, CS_2−$CDCl_3$ (4:1 v/v), or $Cl_2CDCDCl_2$. For measurements in CS_2, a capillary containing C_6D_{12} was used as an external standard. Chemical shifts are reported in ppm relative to tetramethylsilane, using the signals of C_6D_{12} or $CDCl_3$. 1-Alkyl-4-chloro-1,4-dihydro[60]fullerenes (**1a**−**c**) were prepared as described in our previous reports.[3,4] Anhydrous solvents were prepared by standard methods. Other commercially available reagents were of reagent-grade quality and were used as received.

Reaction of 1-Chloro-4-chloromethyl-1,4-dihydro[60]fullerene (1a) with 1,8-Bis(dimethylamino)naphthalene (2). To a solution of **1a** (75.0 mg, 93.1 μmol) in dry CS_2 (15 mL) was added **2** (186 mg, 0.868 mmol) under vigorous stirring in the dark. The mixture was stirred for 3 days at rt in the dark and then concentrated to a volume of about 1 mL. The products were precipitated by the addition of acetone (30 mL) and by ultrasonication for 20 min, giving a dark green solid suspended in a greenish brown solution. The solid was collected by filtration through a PTFE membrane filter of 0.5 μm pore size (81 mg). A part (22 mg) of the solid was separated by HPLC using a "Buckyprep" column (10 mm $\phi \times$ 250 mm) to afford **3a** (8.6 mg, 35%) and **4a** (mixture of meso and racemic diastereomers) (1.1 mg, 5.7%).

3a: dark green solid; mp >300 °C; ^{1}H NMR (CS_2, 400 MHz) δ 2.92 (s, 6H), 2.96 (s, 6H), 4.73 (d, $J = 10.7$ Hz, 1H), 4.80 (d, $J = 10.7$ Hz, 1H), 7.02 (d, $J = 7.5$ Hz, 1H), 7.03 (d, $J = 8.1$ Hz, 1H), 7.42 (dd, $J = 8.5$, 7.5 Hz, 1H), 8.20 (d, $J = 8.1$ Hz, 1H), 9.39 (d, $J = 8.5$ Hz, 1H); ^{13}C NMR (CS_2, 100 MHz) δ 44.4 (2CH_3), 44.7 (2CH_3), 51.1 (CH_2), 59.6, 63.1, 111.9 (CH), 113.5 (CH), 119.4 (CH), 120.6, 126.9 (CH), 129.1 (CH), 132.3, 137.3, 138.8, 139.17, 139.21, 139.9, 141.3, 142.4, 142.46, 142.53, 142.55, 142.93, 142.95, 143.2, 143.3, 143.5 (2C), 143.6, 143.76, 143.79, 143.80, 143.83, 143.85, 143.897, 143.903, 144.2, 144.3, 144.5, 144.57, 144.59, 144.64, 144.8 (2C), 144.88, 144.90, 145.06, 145.10, 145.14, 145.7, 145.8, 145.9, 145.96, 146.02, 147.0, 147.2, 147.26, 147.33, 147.34, 147.4, 147.55, 147.60, 147.9, 148.3, 148.5, 149.00, 149.02, 149.1, 151.3, 151.4, 153.3, 154.2, 156.6; UV−vis (cyclohexane) λ_{max} (ϵ) 209 (183 000), 250 (102 000), 331 (37 100), 447 (6580), 610sh (1920) nm; HRMS (FAB+) calcd for $C_{75}H_{20}ClN_2$ [(M + H)$^+$] m/z 983.1316, found 983.1336.

4a (mixture of meso and racemic diastereomers): brown solid; ^{1}H NMR (CS_2−$CDCl_3$ 4:1 v/v, 300 MHz) δ 4.93 (d, $J = 10.7$ Hz, 1H), 4.97 (d, $J = 10.8$ Hz, 1H), 5.09 (d, $J = 10.8$ Hz, 1H), 5.11 (d, $J = 10.7$ Hz, 1H); UV−vis (cyclohexane) λ_{max} (ϵ) 211 (217 000), 259 (168 000), 447 (14 100) nm; APCI MS (negative ion mode, toluene-CH_3OH 1:1) m/z 1569 ([M + CH_3O]$^-$), 769 ([M/2]$^-$).

Reaction of 1-Chloro-4-dichloromethyl-1,4-dihydro[60]fullerene (1b) with 1,8-Bis(dimethylamino)naphthalene (2). Compound **1b** (72 mg, 86 μmol) was treated with **2** (1.46 g, 6.82 mmol) for 12 h in CS_2 (100 mL) to give a mixture of products as a dark green solid (90 mg). A part (18 mg) of this solid product mixture was separated as described above to afford **3b** (11.8 mg, 68%) and **4b** (0.6 mg, 4%).

3b: dark green solid; mp >300 °C; ^{1}H NMR (CS_2, 400 MHz) δ 2.93 (s, 6H), 2.97 (s, 6H), 6.68 (s, 1H), 7.02 (d, $J = 7.5$ Hz, 1H), 7.03 (d, $J = 8.1$ Hz, 1H), 7.42 (dd, $J = 8.5$, 7.5 Hz, 1H), 8.20 (d, $J = 8.1$ Hz, 1H), 9.34 (d, $J = 8.5$ Hz, 1H); ^{13}C NMR (CS_2, 100 MHz) δ 44.4 (2CH_3), 44.6 (2CH_3), 63.1, 65.4, 76.2 (CH), 111.9 (CH), 113.6 (CH), 119.3 (CH), 120.6, 127.0 (CH), 129.0 (CH), 132.17, 137.2 (2C), 137.7, 139.1 (2C), 141.3, 141.4, 142.1, 142.47, 142.55, 142.6, 142.8, 142.9, 143.1, 143.2, 143.39, 143.43, 143.44, 143.5, 143.67, 143.69, 143.78, 143.81, 143.88, 143.89, 144.0, 144.22, 144.25, 144.5, 144.56, 144.59, 144.79, 144.81, 144.83, 145.0, 145.1, 145.2, 145.3, 145.5, 145.6, 145.7, 146.0, 146.13, 146.15, 147.2, 147.27, 147.34, 147.35, 147.4, 147.6, 147.7, 149.0, 149.1, 149.2, 149.3, 149.5, 150.4, 151.37, 151.43, 153.4, 156.3; UV−vis (cyclohexane) λ_{max} (ϵ) 212 (125 000), 250 (95 400), 331 (34 500), 448 (6100), 610sh (1820) nm; HRMS (FAB+) calcd for $C_{75}H_{19}Cl_2N_2$ [(M + H)$^+$] m/z 1017.0926, found 1017.0928.

4b (mixture of meso and racemic diastereomers): brown solid; ^{1}H NMR (CS_2, 300 MHz) δ 6.98 (s, 1H), 7.05 (s, 1H); UV−vis (cyclohexane) λ_{max} 210, 258, 447 nm; APCI MS (negative ion mode, toluene−CH_3OH 1:1) m/z 1637 ([M + CH_3O]$^-$), 803 ([M/2]$^-$).

Reaction of 1-Chloro-4-trichloromethyl-1,4-dihydro[60]fullerene (1c) with 1,8-Bis(dimethylamino)naphthalene (2). Compound **1c** (80.1 mg, 91.6 μmol) was treated with **2** (974 mg, 4.54 mmol) for 1.5 h in CS_2 (50 mL) to give a mixture of products as a dark green solid (106 mg). Half (53.1 mg) of the solid was separated as described above to afford **3c** (19 mg, 39%) and **4c** (trace amount).

3c: dark green solid; mp >300 °C; ^{1}H NMR (CS_2, 400 MHz) δ 2.90 (s, 6H), 2.92 (s, 6H), 6.94 (d, $J = 8.2$ Hz, 1H), 7.00 (d, $J = 7.5$ Hz, 1H), 7.44 (dd, $J = 8.2$, 7.5 Hz, 1H), 8.15 (d, $J = 8.2$ Hz, 1H), 9.29 (d, $J = 8.2$ Hz, 1H); ^{13}C NMR (CS_2, 100 MHz) δ 44.4, 44.7, 63.8, 73.2, 102.0, 111.7, 113.3, 119.7, 120.2, 126.9, 130.7, 131.6, 137.1, 137.4, 138.5, 139.1, 140.5, 141.0, 141.6, 142.3, 142.8, 142.86, 142.91 (2C), 143.0, 143.08, 143.13, 143.4, 143.5, 143.6, 143.7, 143.81 (2C), 143.85, 144.0, 144.1, 144.3, 144.4, 144.5, 144.56, 144.60, 144.7, 144.8 (2C), 144.9, 145.0, 145.2, 145.3, 145.5, 145.6, 145.7, 146.0, 146.1, 146.21, 147.24, 147.32, 147.34, 147.35, 147.40, 147.6, 147.7, 148.5, 148.9, 149.3, 149.5, 150.8, 150.9, 151.4 (2C), 151.5, 152.8, 155.5, 157.1; UV−vis (cyclohexane) λ_{max} (ϵ) 210 (154 000), 251 (102 000), 330 (37 000), 446 (6100), 610sh (2560) nm; HRMS (FAB+) calcd for $C_{75}H_{18}Cl_3N_2$ [(M + H)$^+$] m/z 1051.0536, found 1051.0525.

Reaction of 1-Chloro-4-dichloromethyl-1,4-dihydro[60]fullerene (1b) with *N,N*-Dimethyl-1-naphthylamine (7). Compound **1b** (22.5 mg, 26.8 μmol) was treated with 46 equiv of **7** (211 mg, 1.23 mmol) in 1,1,2,2-tetrachloroethane (20 mL) for 15 h, and the product mixture was purified as described for **1a** to afford **8** (11.6 mg, 44%) and **4b** (trace amount).

8: dark brown solid; ^{1}H NMR (CS_2−$CDCl_3$ 4:1 v/v, 300 MHz) δ 3.01 (s, 6H), 6.65 (s, 1H), 7.20 (d, $J = 8.1$ Hz, 1H), 7.60 (m, 2H), 8.30 (d, $J = 8.1$ Hz, 1H), 8.40 (d, $J = 8.4$ Hz, 1H), 9.84 (d, $J = 8.4$ Hz, 1H); ^{13}C NMR (CS_2, 99.5 MHz) δ 45.7, 63.0, 65.5, 76.1, 114.2, 125.9, 126.1, 126.3, 126.4, 127.3, 128.7, 129.1, 129.4, 130.3, 133.9, 134.1, 137.7, 138.4, 139.1, 139.2, 141.1, 141.5, 142.1, 142.5, 142.59, 142.63, 142.8, 142.9, 143.1, 143.42, 143.4, 143.48, 143.51, 143.54, 143.72, 143.75, 143.77, 143.81, 143.88, 143.92, 144.1, 144.26, 144.34, 144.5, 144.56, 144.57, 144.79, 144.80, 144.81, 144.99, 145.0, 145.1, 145.18, 145.20, 145.4, 145.7, 146.07, 146.14, 146.2, 147.3, 147.37, 147.38, 147.40, 147.6, 147.7, 148.9, 149.0, 149.2, 149.3, 150.5, 152.4, 153.0; UV−vis (cyclohexane) λ_{max} (ϵ) 210 (98900), 256 (61700), 444 (4100); HRMS (FAB+) calcd for $C_{73}H_{14}Cl_2N$ [$(M + H)^+$] *m*/*z* 974.0504, found 974.0519.

Cyclic Voltammetry. A three-electrode cell, consisting of a BAS 11-2012 glassy carbon working electrode, a Pt wire counter electrode, and a Ag/$AgNO_3$ (0.01 M) reference electrode, was employed. The measurements were carried out at a scan rate of 50 mV/s for 1,2-dichlorobenzene or benzonitrile solutions containing 0.5 mM of sample with 0.05 M of tetrabutylammonium hexafluorophosphate or tetrabutylammonium tetrafluoroborate as a supporting electrolyte. The potentials were calibrated with an internal ferrocene standard.

Calculations. Molecular structures were optimized by DFT calculations at the B3LYP/6-31G(d) level using the Gaussian-98 programs[19] with no symmetry restrictions for **1b**, **2**, and **3b** and with I_h symmetry for C_{60}. Frequency calculations were performed at the B3LYP/6-31G(d) level for **2** and the B3LYP/3-21G* level for **1b**, **3b**, and C_{60}. The latter level, which gave optimized structures similar to those obtained by B3LYP/6-31G(d), was chosen to reduce computational time. The absence of a negative frequency was confirmed for all structures.

Acknowledgment. This work was supported by a Grant-in-Aid for Scientific Research from the Ministry of Education, Culture, Sports, Science and Technology, Japan.

Supporting Information Available: NMR spectra of **3a**−**c**, **4a**,**b**, and **8** and B3LYP/6-31G(d)-optimized structures and total energies of **1b**, **2**, **3b**, and C_{60}. This material is available free of charge via the Internet at http://pubs.acs.org.

JO0351421

---

[18] (a) D'Souza, F.; Caron, C.; Subramanion, R.; Kutner, W.; Jones, M. T.; Kadish, K. M. In *Recent Advances in the Chemistry and Physics of Fullerenes and Related Materials*; Kadish, K. M., Ruoff, R. S., Eds.; The Electrochemical Society: Pennington, NJ, 1994; Vol. 94-24, pp 768−778. (b) Echegoyen, L.; Diederich, F.; Echegoyen, L. E. In *Fullerenes: Chemistry, Physics, and Technology*, Kadish, K. M., Ruoff, R. S., Eds.; Wiley-Interscience: New York, 2000; p 21.

[19] Frisch, M. J.; Trucks, G. W.; Schlegel, H. B.; Scuseria, G. E.; Robb, M. A.; Cheeseman, J. R.; Zakrzewski, V. G.; Montgomery, J. A., Jr.; Stratmann, R. E.; Burant, J. C.; Dapprich, S.; Millam, J. M.; Daniels, A. D.; Kudin, K. N.; Strain, M. C.; Farkas, O.; Tomasi, J.; Barone, V.; Cossi, M.; Cammi, R.; Mennucci, B.; Pomelli, C.; Adamo, C.; Clifford, S.; Ochterski, J.; Petersson, G. A.; Ayala, P. Y.; Cui, Q.; Morokuma, K.; Salvador, P.; Dannenberg, J. J.; Malick, D. K.; Rabuck, A. D.; Raghavachari, K.; Foresman, J. B.; Cioslowski, J.; Ortiz, J. V.; Baboul, A. G.; Stefanov, B. B.; Liu, G.; Liashenko, A.; Piskorz, P.; Komaromi, I.; Gomperts, R.; Martin, R. L.; Fox, D. J.; Keith, T.; Al-Laham, M. A.; Peng, C. Y.; Nanayakkara, A.; Challacombe, M.; Gill, P. M. W.; Johnson, B.; Chen, W.; Wong, M. W.; Andres, J. L.; Gonzalez, C.; Head-Gordon, M.; Replogle, E. S.; Pople, J. A. *Gaussian 98*, Revision A.11; Gaussian, Inc.: Pittsburgh, PA, 2001.